THE JOURNAL OF BIOLOGICAL CHEMISTRY VOL. 283, NO. 38, pp. 26283–26296, September 19, 2008

Differentiated Murine Airway Epithelial Cells Synthesize a Leukocyte-adhesive Hyaluronan Matrix in Response to Endoplasmic Reticulum Stress*[S]

Received for publication, May 1, 2008, and in revised form, July 8, 2008 Published, JBC Papers in Press, July 21, 2008, DOI 10.1074/jbc.M803350200

Mark E. Lauer[‡], Serpil C. Erzurum[§], Durba Mukhopadhyay[‡], Amit Vasanji[‡], Judith Drazba[¶], Aimin Wang[‡], Csaba Fulop[‡], and Vincent C. Hascall[‡1]

From the Departments of [‡]Biomedical Engineering and [§]Pathobiology and the [¶]Imaging Core, Lerner Research Institute, Cleveland Clinic, Cleveland, Ohio 44195

In this report, we describe a novel method for culturing murine trachea epithelial cells on a native basement membrane at an air-liquid interface to produce a pseudostratified, differentiated airway epithelium composed of ciliated and nonciliated cells. This model was used to examine hyaluronan synthesis by the airway epithelial cells (AECs) in response to poly(I,C) and tunicamycin. The former induces a response similar to viral infection, and the latter is a bacterial toxin known to induce endoplasmic reticulum (ER) stress. We found significant accumulation of hyaluronan on the apical surface of the AECs in response to ER stress, but, unlike previously reported results with smooth muscle cells, no increase in hyaluronan was observed in response to poly(I,C). Monocytic U937 cells adhered at 4 °C to the apical surface of the AECs subjected to ER stress by a mechanism almost entirely mediated by hyaluronan. The U937 cells spontaneously released themselves from the abnormal hyaluronan matrix when their metabolism was restored by shifting the temperature from 4 to 37 °C in a custom-made flow chamber. Time lapse confocal microscopy permitted live imaging of this interaction between the U937 cells and the hyaluronan matrix and their subsequent response at 37 °C. Within 45 min, we observed dynamic protrusions of the U937 cell plasma membrane into nearby hyaluronan matrix, resulting in the degradation of this matrix. Simultaneously, we observed some reorganization of the hyaluronan matrix, from a generalized, apical distribution to localized regions around the AEC tight junctions. We discuss the implications these results might have for the airway epithelium and its relation to airway inflammation and hyperresponsiveness associated with asthma and other airway diseases.

The basement membrane (BM)[2] of the airway epithelium is a thin sheet of specialized extracellular matrix that separates the epithelium from underlying mesenchymal cells and provides a protective barrier against pathogens (1). BMs are composed of type IV collagen, various laminin isoforms, and proteoglycans and are unique among other extracellular matrices (2).

Tammi *et al.* (3) described a method in which a native BM could be synthesized by Madin-Darby canine kidney (MDCK) cells and deposited on the apical surface of a native, type I, rat tail collagen gel. They applied rat epidermal keratinocytes to this BM "lift culture" (*i.e.* air-liquid interface) model to produce a well differentiated epidermis. In this report, we applied primary murine airway epithelial cells (AECs) to this MDCK cell-generated BM "lift culture" model and present the advantages of this model compared with current methods.

Hyaluronan is a glycosaminoglycan composed of the repeating disaccharide β1,4-*N*-acetylglucosamine linked β1–3 to glucuronic acid. It typically has an average of $\sim 10^4$ disaccharides with a range of mass from 10^5 to 10^7 Da, and it is the only glycosaminoglycan not attached to a core protein. Hyaluronan is synthesized at the cell surface by one or more of three different hyaluronan synthases (4). Hyaluronan degradation typically occurs by internalization into a unique membrane compartment through a mechanism involving the cell surface receptor CD44 and limited hyaluronidase cleavage. Subsequently, the hyaluronan fragments are transported to lysosomes for complete degradation (5). Hyaluronan may also be degraded externally at sites of inflammation by reactive oxygen species and secreted hyaluronidases of bacterial origin (6).

Hyaluronan has been identified *in vivo* on both the apical (7) and basal (8) surfaces of the airway epithelium. It has also been found in both normal (9) and pathological (10–12) airway secretions. Very little is known about airway epithelial hyaluronan synthesis, especially in the *in vitro* differentiated AEC models currently used (*i.e.* lacking a basement membrane). Using these models, exogenous hyaluronan fragments have been applied to the AECs to study cilia beat frequency (13) and the induction of IL-8 and IL-10 (14). One study used this culture model to describe hyaluronan degradation by reactive oxygen species in apical washes (15).

There is substantial evidence that viral infections trigger and exacerbate asthma and chronic obstructive pulmonary disease (16). The airway epithelium is the principal site of these viral infections. In a model employing a respiratory syncytial virus and a viral mimic (poly(I,C)), smooth muscle cells were shown to produce an abnormal hyaluronan matrix, which permitted

* This work was supported, in whole or in part, by National Institutes of Health Grant PO1 HL081064 Pathology of Asthma. The costs of publication of this article were defrayed in part by the payment of page charges. This article must therefore be hereby marked "*advertisement*" in accordance with 18 U.S.C. Section 1734 solely to indicate this fact.

[S] The on-line version of this article (available at http://www.jbc.org) contains supplemental Figs. S1–S3 and Movies S1–S4.

[1] To whom correspondence should be addressed: Dept. of Biomedical Engineering/ND20, Cleveland Clinic, Cleveland, OH 44195. Tel.: 216-445-5676; Fax: 216-444-9198; E-mail: hascalv@ccf.org.

[2] The abbreviations used are: BM, basement membrane; AEC, airway epithelial cell; ER, endoplasmic reticulum; MDCK, Madin-Darby canine kidney; FBS, fetal bovine serum; PBS, phosphate-buffered saline; HBSS, Hanks' balanced salt solution; DMEM, Dulbecco's modified Eagle's medium.

leukocyte adhesion (17). A similar result was observed when smooth muscle cells were subjected to endoplasmic reticulum (ER) stress (18) also known to be associated with viral infection (19).

In this report, we describe significant hyaluronan accumulation on the apical surface of differentiated AECs in response to tunicamycin. Tunicamycin is a bacterial toxin that inhibits *N*-glycosylation, thus preventing protein folding and inducing ER-stress (20). Also known as the unfolded protein response, or UPR, ER stress refers to a sophisticated network of pathways, resulting in protein translation attenuation, up-regulation of ER chaperones, and the expression of components necessary for ER-associated degradation in response to the accumulation of misfolded proteins in the ER (21). We observed significant leukocyte adhesion to this hyaluronan matrix and present animated evidence of its degradation by these cells using time lapse confocal microscopy.

We also present the unexpected finding that poly(I,C) failed to induce the formation of the abnormal hyaluronan matrix in the AEC model in contrast to the significant hyaluronan response in colon smooth muscle cells (17). Poly(I,C) is a synthetic double-stranded RNA, which can be used to mimic viral infections without the hazards of using a viable virus (22). We discuss the implications this might have for the airway epithelium, its effect on mucus composition and rheology, and the implications for airway inflammation and hyperresponsiveness associated with asthma and other airway diseases.

EXPERIMENTAL PROCEDURES

Preparation of Basement Membranes—This protocol is identical to previous work by Tammi *et al.* (3). Briefly, this protocol involved the formation of a native type I, rat tail collagen gel (354236; BD Biosciences) on the apical surface of tissue culture inserts (657638; Greiner Bio-One). Basement membranes were generated by applying Madin-Darby canine kidney (MDCK) cells to the apical surface of the collagen gel. Three weeks after seeding, the MDCK cells were removed by osmotic and detergent lysis, and the remaining apical matrix covering the surface of the collagen gel has been shown to be a native basement membrane.

Animals and Animal Care—21-Day-old female BALB/c mice were purchased from Charles River (Wilmington, MA) and housed under conditions of constant temperature with 12-h light/dark cycles. Food and water were available *ad libitum*. The mice were sacrificed by administering Nembutal (Ovation Pharmaceuticals, Deerfield, IL) at 0.125 mg/g of mouse weight. All protocols with the animals were approved by the Cleveland Clinic Institutional Animal Care and Use Committee.

Primary Cell Culture—This protocol was essentially identical to previous work by You *et al.* (23). After sacrifice, the tracheas were excised from the mice and placed in Ham's F-12 nutrient medium with 50 units/ml penicillin, 50 μg/ml streptomycin and maintained at 4 °C on ice. Under a dissecting microscope, the esophagus and surrounding connective tissue were removed. The tracheas were cut longitudinally with a scalpel to expose the lumen and transferred to 5 ml of 0.15% pronase (10165921001; Roche Applied Science) in Ham's F-12 nutrient medium with 50 units/ml penicillin and 50 μg/ml streptomycin for an overnight incubation at 4 °C in a 15-ml centrifuge tube. The next day, fetal bovine serum (FBS) was added to the tracheas (final concentration 10%), inhibiting further protease degradation. The medium, containing the released epithelial cells, was transferred to a 50-ml centrifuge tube. Washing medium (5 ml), containing Ham's F-12 nutrient medium with 50 units/ml penicillin, 50 μg/ml streptomycin, and 10% FBS, was added to the tracheas. The 15-ml centrifuge tube, containing the tracheas, was inverted several times to dislodge remaining epithelial cells. The supernatant was pooled with the original isolate, and the washing step was repeated twice, pooling all supernatents. Afterward, the tracheas were brushed with a cotton swab in a 100-cm^2 Petri dish, containing 5 ml of washing medium, to remove remaining adherent epithelial cells, pooling all supernatants. This was repeated twice. The remaining tracheas were cut into small pieces (typically 30 pieces/trachea), and transferred to a 100-cm^2 Petri dish for attachment and outgrowth of smooth muscle cells for a separate study. The pooled epithelial supernatants were centrifuged at 300 $\times$ *g* for 10 min. The pellet was resuspended in 2 ml of Ham's F-12 nutrient medium with 50 units/ml penicillin, 50 μg/ml streptomycin, 10 mg/ml bovine serum albumin (BSA) (BP-1605-100; Fisher), and pancreatic DNase I (0.5 mg/ml) (DN-25; Sigma) for 5 min on ice and centrifuged at 300 $\times$ *g* for 5 min. The pellet was resuspended in 12 ml of DMEM/F-12 with 100 units/ml penicillin, 100 μg/ml streptomycin, 0.25 μg/ml amphotericin B, 20 mM L-glutamine, and 10% FBS and transferred to a 100-cm^2 Primaria^{TM} Petri dish (353803; BD Biosciences). Debris was removed with fine forceps, and the remaining isolate was incubated at 37 °C, 5% CO_2, and 100% humidity for 3 h to allow for the attachment of any contaminant smooth muscle cells or fibroblasts. Afterward, the culturing medium, containing the nonadherent epithelial cells, was transferred to a 50-ml tube. The adherent cells were washed once with 12 ml of medium to remove remaining nonadherent epithelial cells and pooled with the first isolate. The purified epithelial cells were centrifuged at 300 $\times$ *g* for 10 min. The pellet was resuspended at 100,000 cells/ml in DMEM/F-12 medium containing 100 units/ml penicillin, 100 μg/ml streptomycin, 0.25 μg/ml amphotericin B, 20 mM L-glutamine, 5 mM glucose, 5% FBS, 10 μg/ml insulin (I-6634; Sigma), 5 μg/ml transferrin (T-1147; Sigma), 0.1 μg/ml cholera toxin (C-8052; Sigma), 25 ng/ml epidermal growth factor (354001; BD Biosciences), 30 μg/ml bovine pituitary extract (P-1476; Sigma), and 80 nM retinoic acid (R-2625; Sigma). The cells were seeded onto the basement membrane-covered tissue culture inserts at 443,000 cells/cm^2 (200,000 cells/well of a 6-well plate or 50,000 cells/well of a 12-well plate).

The remaining culture of the epithelial cells differed from You *et al.* (23) in the following ways. We seeded the epithelial cells onto basement membrane-covered tissue culture inserts, as opposed to seeding them on inserts coated with a type I rat tail collagen alone. Our seeding density was 443,000 cells/cm^2 (200,000 cells/well of a 6-well plate, or 50,000 cells/well of a 12-well plate). This seeding density was 40% less than the minimum suggested by You *et al.* We found that seeding fewer cells/well resulted in a less differentiated, cuboidal-to-squamous phenotype. Seeding more cells resulted in cell stratification. Our ability to seed fewer cells than previously described is

probably due to enhanced binding efficiency associated with the basement membrane (Fig. 1). Additionally, we found that standard DMEM/F-12 with 13.5 mM glucose resulted in abnormal cell stratification during the differentiation period when compared with cells grown in DMEM/F-12 with 5 mM glucose. For this reason, our cells were cultured in 5 mM glucose (physiological levels) with medium replacement every other day. We noticed that hyaluronan accumulated on the apical surface of the epithelial cells during the differentiation period. A significant amount of this hyaluronan could be washed away by rinsing the apical surface with fresh medium. Since the accumulation of hyaluronan on the apical surface would adversely affect our assays, we washed the apical surface at each feeding.

Toluidine Blue Light Microscopy—At the time of harvest, the epithelial cells were gently washed with 37 °C equilibrated PBS and fixed with 2.5% gluteraldehyde and 4% paraformaldehyde at pH 7.3 at 4 °C overnight. Sections (1 × 1 mm) of the cells (on the collagen gel and on the basement membrane) were cut out of the entire culture insert, making sure that the porous membrane of the culture insert was detached from the collagen gel (failure to do this will prevent smooth sectioning). The cells were washed three times in 4 °C sodium cacodylate buffer (0.2 M, pH 7.3), and a plastic pipette was used to apply 1% osmium tetroxide (in water) to the cells in a fume hood. After a 1-h incubation, the samples were washed with the sodium cacodylate buffer twice, rinsed with maleate buffer once (0.2 M, pH 5.1), and stained with 1% uranyl acetate (in maleate buffer) for 60 min. The cells were washed with maleate buffer and dehydrated in 50, 70, 95, and 100% ethanol, followed by three washes with propylene oxide. The cells were embedded using the Eponate 12™ kit (18012; Ted Pella, Redding, CA). Sections (1 μm) were cut with a diamond knife on a microtone and attached to a glass slide by heating the slide on a hot plate (low heat) for 3–5 s. Toluidine blue (100 μl of 4% stain in 1% sodium borate) was applied to each section, and the slide was briefly (3–5 s) applied to a hot plate (low heat). The sections were washed in water, air-dried, and mounted with a coverslip.

Experimental Culture—Polyinosinic-polycytidylic acid (poly(I,C)) (P0913; Sigma) and tunicamycin (T7765; Sigma) were applied at 10 and 5 μg/ml, respectively. Treatment duration was 18 h. Two ml of the diluted toxins was added to the basal chamber of one well of a 6-well plate, and 1 ml was added to the apical surface. Although this briefly compromised the air-liquid interface during the treatment interval (18 h), the small volume of medium on the apical surface (~1 mm thick) provided a hydrated environment, similar to the hydration provided by a mucus coat (apparently absent in our model; see Fig. 4) and more suitable for hyaluronan synthesis.

Leukocyte Adhesion Assay—The use of monocytic (macrophage precursor) U937 lymphoma cells (24) for hyaluronan-based leukocyte adhesion assays has been previously reported (17). Ordinarily, 30 million U937 cells (American Type Tissue Culture, Manassas, VA) were labeled with the lipophilic carbocyanine dye CM-DiI (V-22888; Invitrogen) in 30 ml of serum-free RPMI 1640 at 5 μM for 20 min at 37 °C. Afterward, the U937 cells were centrifuged at 300 × *g* for 10 min. The pellet was washed with 10 ml of RPMI 1640 and centrifuged at 300 × *g* for 5 min. This washing step was repeated once. The labeled U937 cells were resuspended in 7.5 ml of ice-cold serum-free DMEM/F-12, supplemented as described by You *et al.* (17) for differentiated growth of the AECs and incubated on ice for 20 min. Commensurate with this time, the conditioned medium of epithelial cell cultures that had been incubated for 18 h with or without the toxins was removed, and both the basal and apical surfaces of the epithelial cells were washed with 37 °C growth medium. Afterward, ice-cold growth medium was applied to the cells (3 and 2 ml basal and apical, respectively), and the epithelial cells were incubated in a room equilibrated to 4 °C for 30 min. The ice-cold, DiI-labeled U937 cells were applied to the ice-cold epithelial cells and maintained at 4 °C for the duration of the experiment. The U937 cells were allowed to settle, by gravity, onto the apical surface of the epithelial cells for 30 min. We found that washing unbound U937 cells directly in the tissue culture insert gave sporadic results caused by the shearing of U937 cells bound to hyaluronan when rinsing medium was directly dripped onto the apical surface with a serological pipette. To avert this, the apical medium (containing the U937 cells) was aspirated, and the collagen gels were cut out of their wells with a scalpel and transferred to the empty wells of a 6-well plate. Washing was accomplished by applying 2 ml of ice-cold DMEM/F-12 to the extreme periphery of each well, avoiding direct dispensing of the washing medium onto the apical surface of the epithelial/U937 cells. Once applied, the plate was gently agitated in a circular motion to remove nonadherent U937 cells, and the supernatant was aspirated. This washing step was repeated four times. U937 cells, bound to hyaluronan, were removed by the application of 0.5 turbidity units/ml *Streptomyces* hyaluronidase (100740-1; Seikagaku, East Falmouth, MA) in ice-cold PBS at 0.5 ml/well for 1 min with occasional agitation and transferred to a 1.5-ml centrifuge tube. This hyaluronidase digestion was repeated one more time, pooling both extracts. U937 cells remaining bound to the cell layer were removed by lysis with 0.5 ml of 1% Triton X-100 in PBS for 5 min at room temperature. This detergent lysis was repeated once, pooling both lysates. The U937 cells released by hyaluronidase were lysed by adding 10 μl of Triton X-100 to each 1 ml of extract and incubating at room temperature for 5 min (final concentration, 1%). The detergent and hyaluronidase extracts were transferred (250 μl each) to a 96-well plate. An aliquot of a known number of labeled U937 cells was also lysed with 1% Triton X-100 and applied to the plate. The number of U937 cells bound was quantified by measuring the extracts on a fluorometer (Cytofluor™ II Fluorescence Multi-Well Reader, Applied Biosystems, Framingham, MA) with excitation and emission at 520 and 590 nm, respectively.

Flow Chamber Assay—U937 cells were applied to the epithelial cells as described for the leukocyte adhesion assay. After removal of the unbound U937 cells, the collagen gel, containing the epithelial and U937 cells, was transferred to a custom-made, open system flow chamber that had been preequilibrated to 4 °C on ice. Ice-cold DMEM/F-12 medium was permitted to flow over the cells by gravity at about 100 ml/min (over a 20-cm^2 surface area), whereas phase-contrast images were taken every 0.5 s using a Leica DMIRB microscope (Heidelberg, Germany) equipped with a CoolSnap™ HQ camera (Roper Scientific, Tucson, AZ) operated by Metamorph software (ver-

sion 6.3, Molecular Devices, Sunnyvale, CA). Medium flow was stopped after 1 min of uninterrupted flow, and 5 ml of *Streptomyces* hyaluronidase was gently applied to the cells at 0.5 turbidity units/ml. Digestion of hyaluronan was permitted for 1 min, followed by resumption of medium flow at the same rate as before application of the enzyme. U937 cells bound to hyaluronan were washed away. In a separate experiment (lacking hyaluronidase), ice-cold medium was applied for 2 min, at about 100 ml/min, followed by the addition of medium equilibrated to 37 °C for an additional 8 min at the same flow rate (Fig. 9). AVI movie sequences were generated using ImagePro Plus (version 6.1, Media Cybernetics, Bethesda, MD), and the files were compressed using Cinepak Codec by Radius.

Live Confocal Assay—U937 cells were applied to the epithelial cells as described for the leukocyte adhesion assay. All of the following procedures were performed in a room that was refrigerated to 4 °C, and all solutions applied to the cells were ice-cold. After removal of the unbound U937 cells, hyaluronan was visualized by applying a biotinylated hyaluronan binding protein (385911; EMD Chemicals, Gibbstown, NJ) at 5 μg/ml in epithelial growth medium for 30 min, followed by four brief washes with epithelium growth medium. Streptavidin, Alexa Fluor® 488 (product S11223; Invitrogen) was applied at 1:500 in epithelial growth medium for 30 min and washed as before. The cells were brought to the confocal microscope on ice, where the collagen gel, containing the epithelial and U937 cells, was transferred to a room temperature glass slide. Ice-cold epithelial growth medium (0.2 ml) was added to the apical surface, and a coverslip was gently applied to the top of the cells. Specimens were imaged at room temperature using a HCX PL APO ×40/1.25 numerical aperture oil immersion objective on a Leica TCS-SP2 confocal microscope (Leica Microsystems, GmbH, Wetzlar, Germany). Z-stacks of images were collected along a 20-μm depth every 5 min for 90 min. During this time, the U937 cells gradually warmed to room temperature (probably by 30 min, as determined by enhanced activity of the U937 cells; see Fig. 10). The live cells were discarded after imaging. AVI movie sequences were generated from the maximized, overlaid images using ImagePro Plus software (see Fig. 10). This same protocol was used to generate the images in Fig. 4 in the absence of U937 cells. For Figs. 4 and 7, all of the images were taken within the first 30 min at room temperature, before peak metabolism was reached.

Hyaluronan Quantification—Live epithelial extracellular hyaluronan was labeled with a biotinylated hyaluronan-binding protein (EMD Chemicals) at 4 °C for 30 min and washed four times with ice-cold growth medium, as described for live confocal imaging. The biotinylated hyaluronan-binding protein was conjugated to streptavidin, labeled with Alexa Fluor® 488 (Invitrogen). This fluorophore was released by the addition of 0.5 ml of 0.5 turbidity units/ml *Streptomyces* hyaluronidase (in ice-cold PBS) to the apical surface of the epithelial cells for 1 min and transferred to a separate tube. This hyaluronidase extraction was repeated once, pooling both extracts, and an aliquot of these extracts was measured on a Cytofluor™ II fluorometer.

Immunohistochemistry—The epithelial cells were fixed in 4% paraformaldehyde in PBS at room temperature for 30 min. The collagen gels (containing the epithelial cells) were cut away from the culturing insert and transferred to a 4-well plate (176740; Nunc, Naperville, IL) to minimize the amount of applied antibody. The cells were rinsed with Hank's balanced salt solution (HBSS) three times and permeablized with 0.1% Triton X-100 in precooled HBSS at 4 °C for 5 min. The cells were washed three times with HBSS and blocked with 1% bovine serum albumin (BP-1605-100; Fisher) in HBSS. A β-tubulin IV antibody (MU178-MC; BioGenex, San Ramon, CA) was applied to the apical surface of the cells at 1:100 dilution in HBSS with 1% bovine serum albumin for 1 h at room temperature. The cells were washed four times with HBSS, and a secondary antibody, conjugated to CY2, was applied at 1:200 for 45 min (115-225-166; Jackson Immunoresearch, West Grove, PA). The cells were washed five times with HBSS, and the collagen gels, containing the cells, were transferred to a glass slide. Vectashield® (H-1200; Vector Laboratories, Burlingame, CA) was applied to the apical surface of the cells followed by applying a 24 × 50-mm coverslip (12–545-F; Fisher). The ciliated cells were visualized by confocal microscopy (TCS-SP2; Leica), scanning 50-μm depth at a step size of 1 μm. Three-dimensional images were generated using Volocity® software (version 4.0.1; Improvision, Inc., Lexington, MA).

Western Blot—As a positive control, primary murine tracheal smooth muscle cells were cultured in DMEM/F-12 medium (10% FBS) at 80% confluence in 6-well plates, treated with the toxins at the same concentrations as described for the epithelial cells, and harvested in the same manner. At the time of epithelial cell harvest, media from the upper and lower chambers were aspirated, and the 12-well culture inserts were transferred to a new 12-well plate. The apical surface of the cells was rinsed with 0.5 ml of 37 °C equilibrated PBS, and the cells were harvested with 0.15 ml of M-PER® Mammalian Protein Extraction Reagent (78501; Pierce) containing Halt™ protease inhibitor mixture (78415; Pierce) applied to the apical surface and incubated at room temperature for 10 min. During this time, the extract solution gradually drained into the basal chamber. When this occurred, the extract was transferred back to the apical surface. This transfer was repeated four times over the 10-min incubation. The protein extraction was transferred to a 1.5-ml tube, and the protein content was quantified using the Micro-BCA™ protein assay kit (23235; Pierce), yielding about 2 mg/ml for each sample. Sample protein (5 μg) was added to each well of a 10-well polyacrylamide gel (NP0321BOX; Invitrogen) and blotted to nitrocellulose (926-31090; Li-Cor, Lincoln, NE). The blot was blocked for 1 h (927-40000; Li-Cor), simultaneously probed with antibodies against KDEL at 1:500 (PA1-013; Affinity Bioreagents, Golden, CO) and β-actin at 1:2,000 (A5441; Sigma) in the blocking buffer with 0.1% Tween 20 for 1 h. In separate blots, the KDEL antibody was substituted with an antibody against VCAM-1 (vascular cell adhesion molecule-1) at 1:100 (sc-8304; Santa Cruz Biotechnology, Santa Cruz, CA). The blots were washed five times in PBS with 0.1% Tween 20 and simultaneously probed with IRDYE secondary antibodies (926-32211 and 926-32222; Li-Cor) at a 1:15,000 dilution in blocking buffer with 0.1% Tween 20 and 0.01% lauryl sulfate for 45 min. The blots were washed as before and imaged on an Odyssey Infrared Imaging System (Li-Cor).

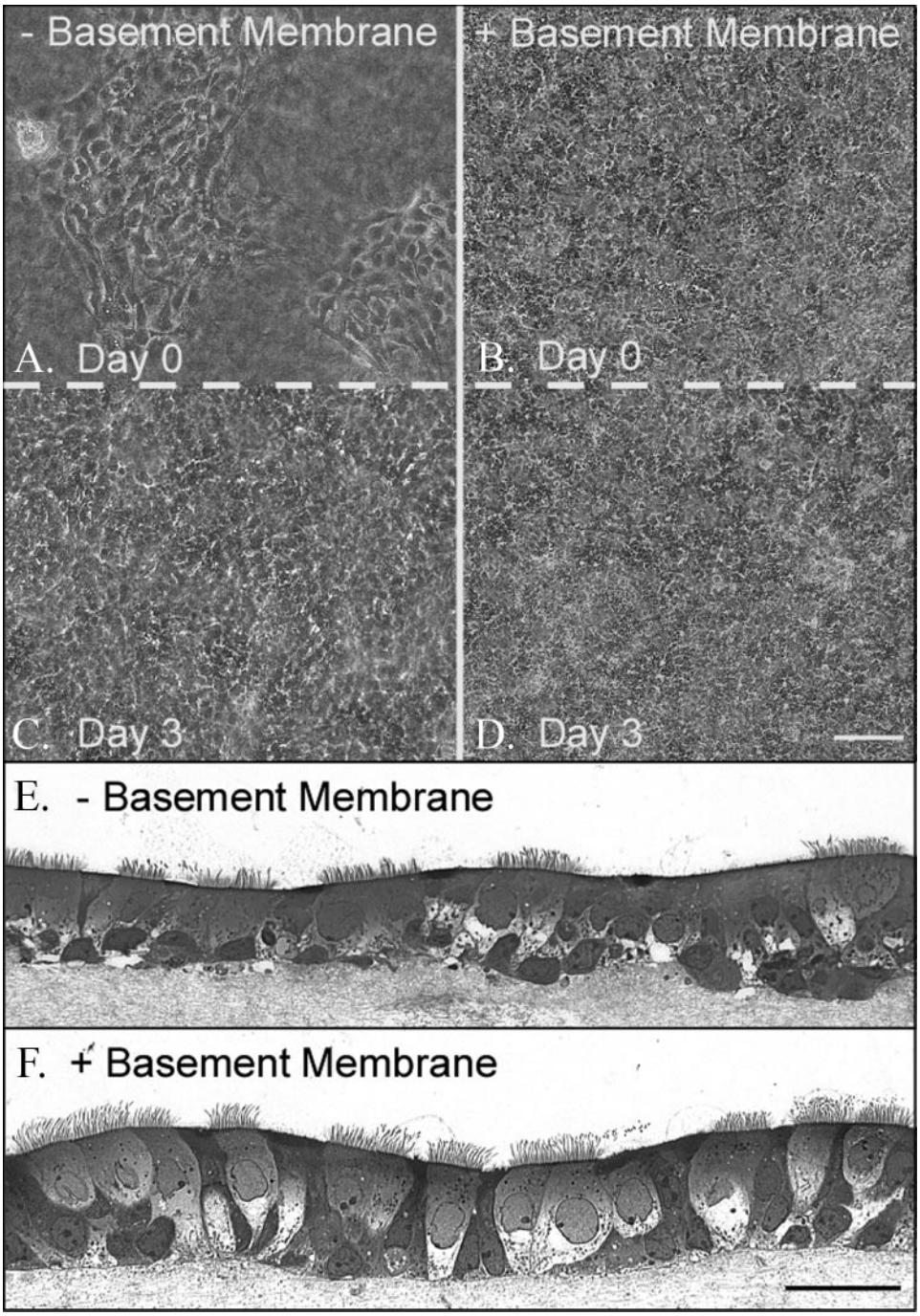

FIGURE 1. **Murine airway epithelial cell morphology when cultured on a native basement membrane compared with a native collagen gel.** Epithelial cells were seeded, at the same density, in culture inserts containing BM (*B*, *D*, and *F*) or on a collagen gel (*A*, *C*, and *E*) (for *A–D*, magnificaton is ×10, and *magnificaton bar* is 100 μm for *A–D*; for *E–F*, magnification is ×40, and the *magnificaton bar* is 100 μm). The day after seeding (day 0), a confluent monolayer of cells was observed on the BM (*B*), whereas patches of cells were observed on the collagen gel (*A*). Three days later, the patches of cells on the collagen gel spread out to confluence (*C*), whereas the cells on the BM showed little change from day 0 (*D*). This experiment was repeated three times. Two weeks later, the epithelial cells cultured on a BM (*F*) were a ciliated, pseudostratified, confluent monolayer portraying a regular basal surface. Cells cultured on a collagen gel (*E*) were also ciliated and mostly pseudostratified, but the confluence showed some multilayer stratification and an irregular basal surface in the absence of the BM.

RESULTS

Differentiated Murine Airway Epithelial Cells Cultured on a Basement Membrane—Equal numbers of AECs were directly applied to a substrata of rat tail native, type I collagen, or applied to the collagen substrata previously covered with a native BM synthesized by MDCK cells. Confluence on the collagen substrata alone was ~25% the day after seeding, where most of the cells were observed in random, confluent patches (Fig. 1*A*). Confluence on the BM was 100% and was uniform in its distribution (Fig. 1*B*). Three days later, the cells on the collagen substrata, alone, reached confluence (Fig. 1*C*), although their density did not appear as high as the cells seeded on the BM (Fig. 1*D*). On day 3, the cells were exposed to an air-liquid interface for differentiation. Two weeks later, transverse sections of the cultures were prepared and stained with toluidine blue. Cells cultured on both the collagen substrata (Fig. 1*E*) and the BM (Fig. 1*F*) gave evidence of differentiation, including the presence of cilia and pseudostratification. Cells cultured on the BM displayed uniform continuity on their basal surface in the regions where they came in contact with the supporting BM matrix (Fig 1*F*). In contrast, cells cultured on the collagen substrata, alone, possessed an irregular basal surface, with cells protruding into the collagen substrata (Fig. 1*E*). For this reason, our epithelial cells were cultured on BMs for the remainder of the report.

We cultured the AECs on BMs and prepared toluidine blue-stained transverse sections 0, 3, 5, 7, 10, and 14 days after exposure to an air-liquid interface (Fig. 2, *A–F*, respectively). On day 0 (3 days after initial seeding and culturing in a submerged state), the cells were a squamous monolayer (Fig. 2*A*), becoming cuboidal by day 3 (Fig. 2*B*). A small percentage of cilia were apparent by day 5 (Fig. 2*C*), reaching a plateau between days 10 and 14 (Fig. 2, *E* and *F*, respectively). Similarly, mature pseudostratification was evident during this interval. Cells in culture >14 days possessed regions of multiple-layered stratification (not shown). For this reason, our epithelial cells were harvested between days 10 and 14 for the remainder of the report.

Differentiated AECs (day 14) were probed with an antibody against β-tubulin IV (green; present in cilia) and imaged by

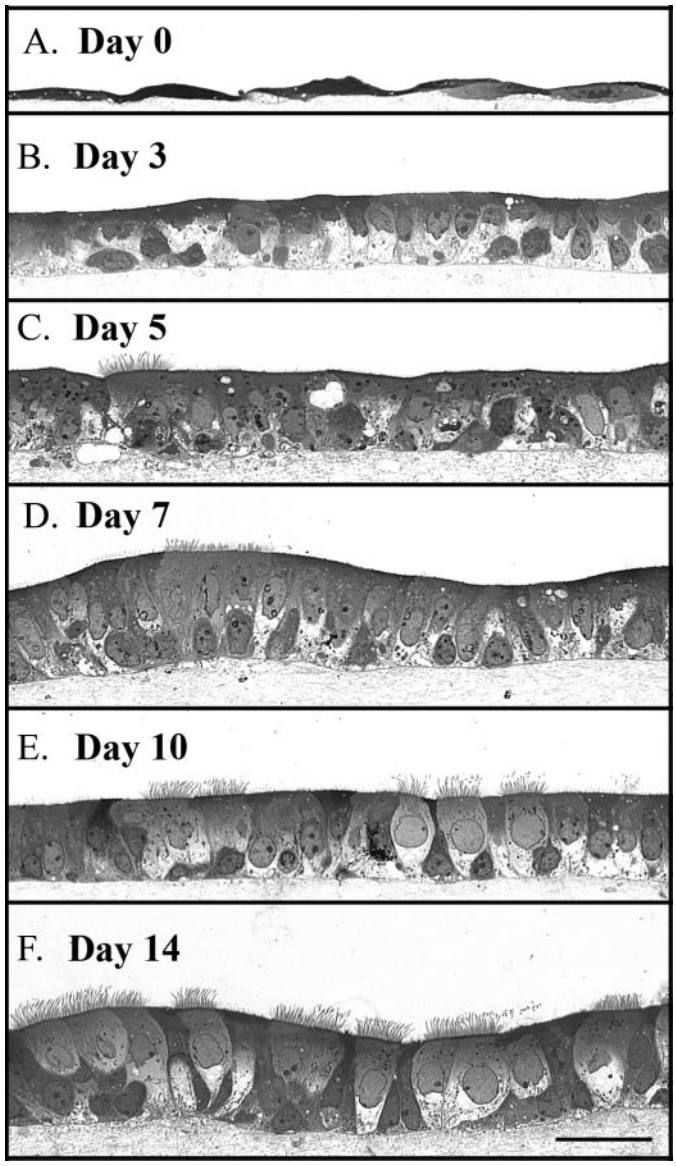

FIGURE 2. **Murine airway epithelial cell differentiation time course on a native basement membrane.** Epithelial cells were harvested 0, 3, 5, 7, 10, and 14 days after exposure to an air-liquid interface (*A–F*, respectively). Differentiation progressed from squamous (day 0) to cuboidal (day 3) to pseudostratified (days 5–14). Cilia formation was apparent by day 5 and reached a plateau between 10 and 14 days. Magnification is ×40. *Magnification bar*, 100 μm.

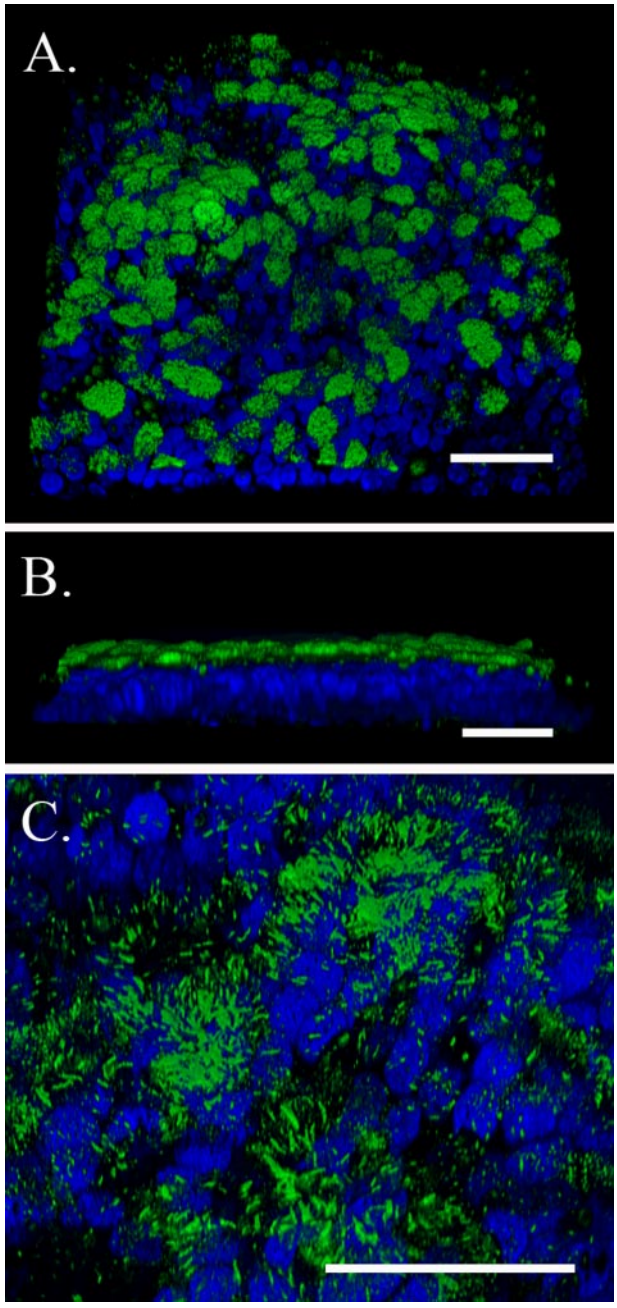

FIGURE 3. **Three-dimensional confocal images of differentiated murine airway epithelial cells cultured on a native basement membrane.** Cilia are highlighted by β-tubulin IV staining (*green*), and DAPI-stained nuclei are *blue*. *A*, the apical surface of the epithelial cells (magnification is ×63). *B*, a lateral cross-section of the epithelial cells (magnification is ×63). *C*, the apical surface zoomed from ×63 to ×~160, where the gain for the green channel was lowered to highlight individual cilia. All *magnification bars* are 50 μm. This experiment was repeated >10 times.

confocal microscopy. Three-dimensional images were generated to illustrate the quality and extent of the cilia (Fig. 3). Fig. 3*A* (×63) portrays the apical surface of the epithelial cells, revealing that ~60% of the cells were ciliated. Fig. 3*B* (×63) shows a transverse view of the epithelial cells, illustrating the overall apical distribution and height of the cilia. Fig. 3*C* presents a higher magnification (×~160) of the apical, epithelial surface, where the gain of the green confocal channel was lowered to better highlight individual cilia. Most of the cilia were ~10 μm in length, although a small percentage were <5 μm.

Pathological Hyaluronan Synthesis by Airway Epithelial Cells in Response to ER Stress—Differentiated AECs (day 14) were treated with poly(I,C) to mimic a viral response or with tunicamycin, a toxin known to induce ER stress. Hyaluronan was visualized by the application of a fluorescence-tagged streptavidin bound to biotinylated hyaluronan-binding protein at 4 °C. Subsequently, the cells were imaged live on a confocal microscope (Fig. 4). Tunicamycin (Fig. 4*C*) induced significant ($p < 0.0003$) hyaluronan accumulation on the apical surface of the epithelial cells when compared with untreated cells (Fig. 4*A*) or cells treated with poly(I,C) (Fig. 4*B*). The amount of hyaluronan present on the external surface of the epithelial cells was quantified by digesting the fluorescent labeled hyaluronan matrix

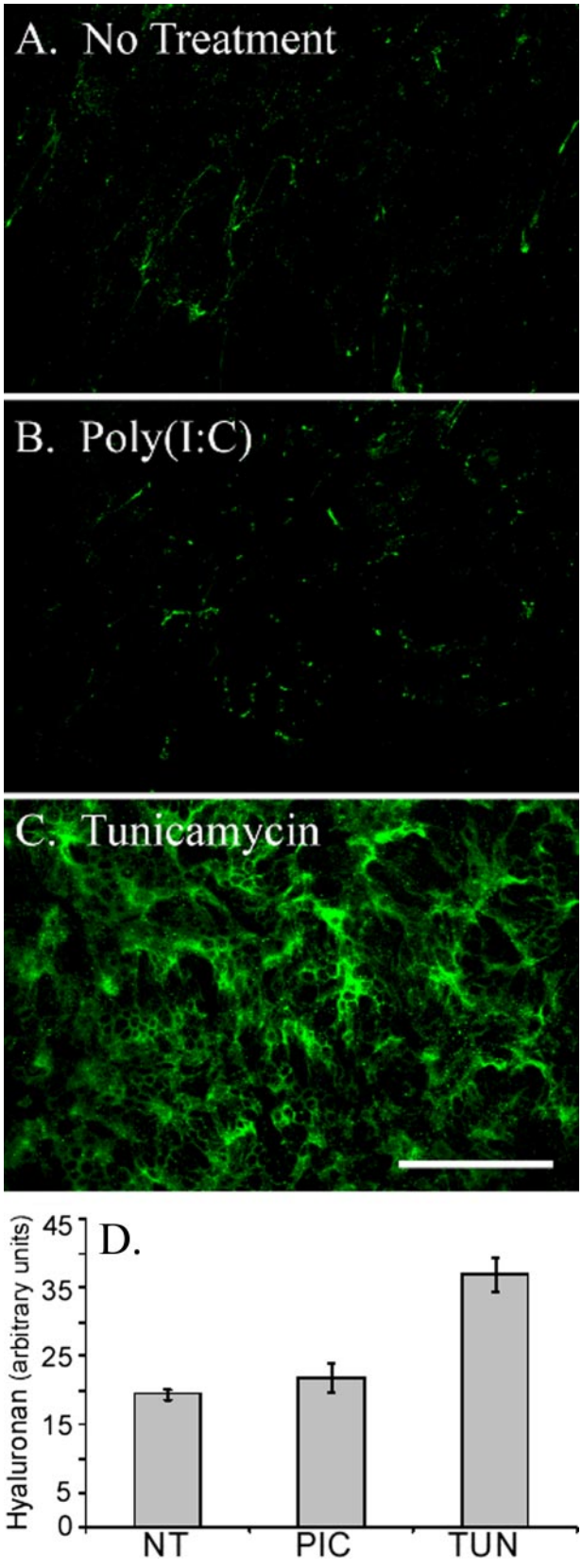

FIGURE 4. **Differentiated murine airway epithelial cells produce hyaluronan on their apical surface in response to tunicamycin but not poly(I,C).** The epithelial cells were treated without (*A*) or with poly(I,C) (*B*) or tunicamycin (*C*) for 18 h and processed for confocal microscopy while still alive. Significant amounts of hyaluronan (*green*) accumulated on the apical surface of the epithelial cells, treated with tunicamycin, when compared with the untreated (*A*) or poly(I,C)-treated (*B*) cells. This experiment was repeated four times. Magnification is ×40. *Magnification bar*, 100 μm. The hyaluronan of untreated (*NT*), poly(I,C)-treated (*PIC*), or tunicamycin-treated (*TUN*) epithelial cells was labeled with biotinylated hyaluronan-binding protein and streptavidin Alexa Fluor® 488 nm. This labeled hyaluronan was digested with *Streptomyces* hyaluronidase to remove extracellular hyaluronan, and the extracts were measured on a fluorometer (*D*). *Error bars*, S.D. ($n = 3$).

with *Streptomyces* hyaluronidase and measuring the extract on a fluorometer (Fig. 4*D*). Despite previous observations that both poly(I,C) and tunicamycin are potent inducers of hyaluronan synthesis by colon and aortic smooth muscle cells (17, 18), AECs failed to increase the synthesis of hyaluronan in response to poly(I,C). It should also be noted that neither poly(I,C) nor tunicamycin induced significant secretion of hyaluronan into the basal medium or released significant amounts from the apical surface (Fig. S1).

Since the differentiated AECs failed to induce the hyaluronan synthesis observed by smooth muscle cells, we were interested to learn if this failure was limited to hyaluronan synthesis or whether other responses, known to be affected by poly(I,C), were intact. Pertinent to leukocyte adhesion, VCAM-1 has been shown to be induced by poly(I,C) in smooth muscle cells (17). Protein extracts, from both murine airway smooth muscle cells and our murine AECs, were analyzed via Western blot. The blots were probed with antibodies against the tetrapeptide KDEL (present on the carboxyl terminus of ER chaperones and known to increase in ER stress) and VCAM-1. Both the airway smooth muscle and epithelial cells primarily expressed a single KDEL-containing protein at about 78 kDa (probably BiP) (*green*; Fig. 5*A*). A nonspecific band (about 37 kDa) was observed in the smooth muscle cell cultures when their blots were probed with the antibody against VCAM-1 (*green*; Fig. 5*B*), but this band did not change in any of the treatment groups, unlike the band at the expected molecular mass for VCAM-1 (110 kDa) (*green*; Fig. 5*B*).

Smooth muscle cells treated with tunicamycin, induced KDEL (*green*; Fig. 5*A*, *lane 3*) when compared with cells treated with poly(I,C) (*lane 2*, $p < 0.003$) or untreated (*lane 1*, $p < 0.001$). Epithelial cell induction of KDEL by tunicamycin (Fig. 5*A*, *lane 6*) was modest when compared with untreated cells (*lane 4*, $p < 0.2$), and treatment with poly(I,C) gave an unexpected decrease in KDEL expression (*lane 5*) when compared with untreated ($p < 0.01$) or tunicamycin-treated ($p < 0.01$) cells.

As expected, VCAM-1 induction by poly(I,C) was observed in the smooth muscle cells (*green*; Fig. 5*B*, *lane 2*) when compared with cells treated with tunicamycin (*lane 3*; $p < 0.001$) or untreated (*lane 1*; $p < 0.001$). In contrast, poly(I,C) did not induce VCAM-1 production by the epithelial cells (*lane 5*).

The quantification of KDEL and VCAM-1 expression is presented in Fig. 5 (*C* and *D*, respectively; $n = 3$). The failure of the epithelial cells to up-regulate VCAM-1 in response to poly(I,C), despite its up-regulation in smooth muscle cells, gives credibility to our unexpected observation that this toxin also fails to induce the accumulation of hyaluronan on the apical surface of the epithelial cells (Fig. 4). We also observed that A23187 (a calcium ionophore) and thapsigargin (an ER calcium ATPase

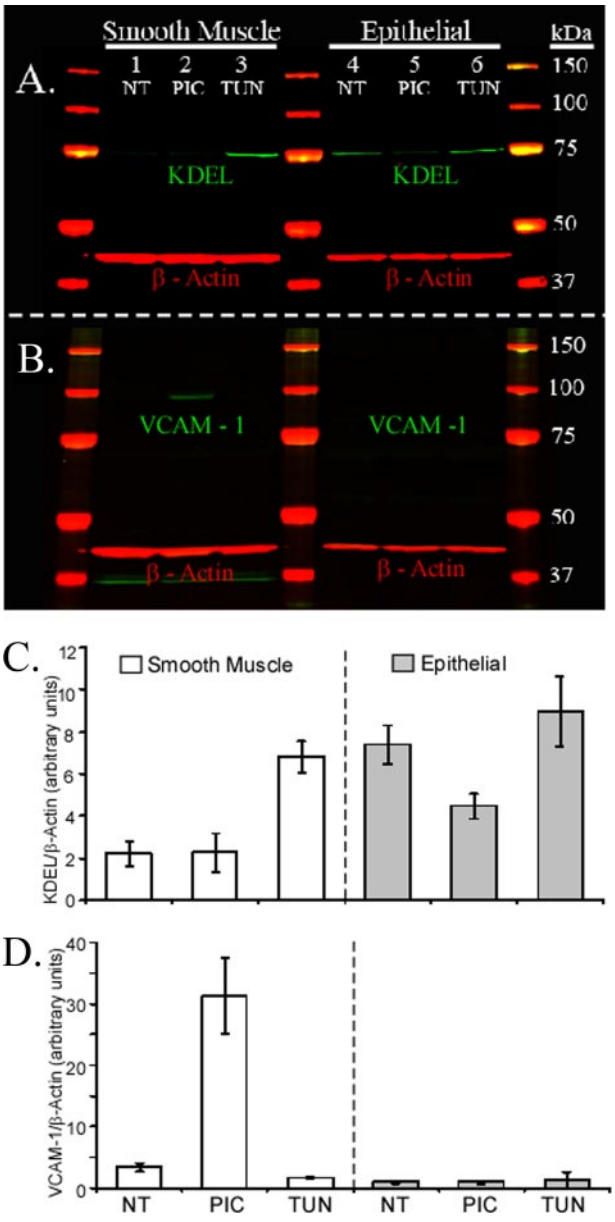

FIGURE 5. **Differential VCAM-1 production between murine airway smooth muscle and epithelial cells in response to poly(I,C).** Airway smooth muscle and epithelial cells were treated without (*NT*; *lanes 1* and *4*) or with poly(I,C) (*PIC*; *lanes 2* and *5*) or tunicamycin (*TUN*; *lanes 3* and *6*). These blots were probed with antibodies against KDEL (*A*, *green*) and VCAM-1 (*B*, *green*). Molecular weight ladders are shown in *red/yellow*. β-Actin (*red*) is shown for each lane as a loading control. The KDEL and VCAM bands (*A* and *B*, respectively) were quantified and presented in *C* and *D*, respectively. *Error bars*, S.D. ($n = 3$).

inhibitor), both known to induce ER-stress, induced hyaluronan synthesis in a manner identical to tunicamycin (Fig. S2).

The expression of KDEL by unstimulated epithelial cells was 3-fold higher than unstimulated smooth muscle cells ($p < 0.001$) when normalized by β-actin (Fig. 5*C*). Previous to this experiment, we had noticed that the epithelium of small airways in the mouse lung (Fig. 6*A*) and trachea (Fig. 6*B*) always presented a strong signal for KDEL (*red*) when compared with other cells. For example, the small bronchiole airway epithelium in Fig. 6*A* (*arrowheads*) portrays a significantly higher KDEL expression than nearby alveolar cells (*pound signs*) or

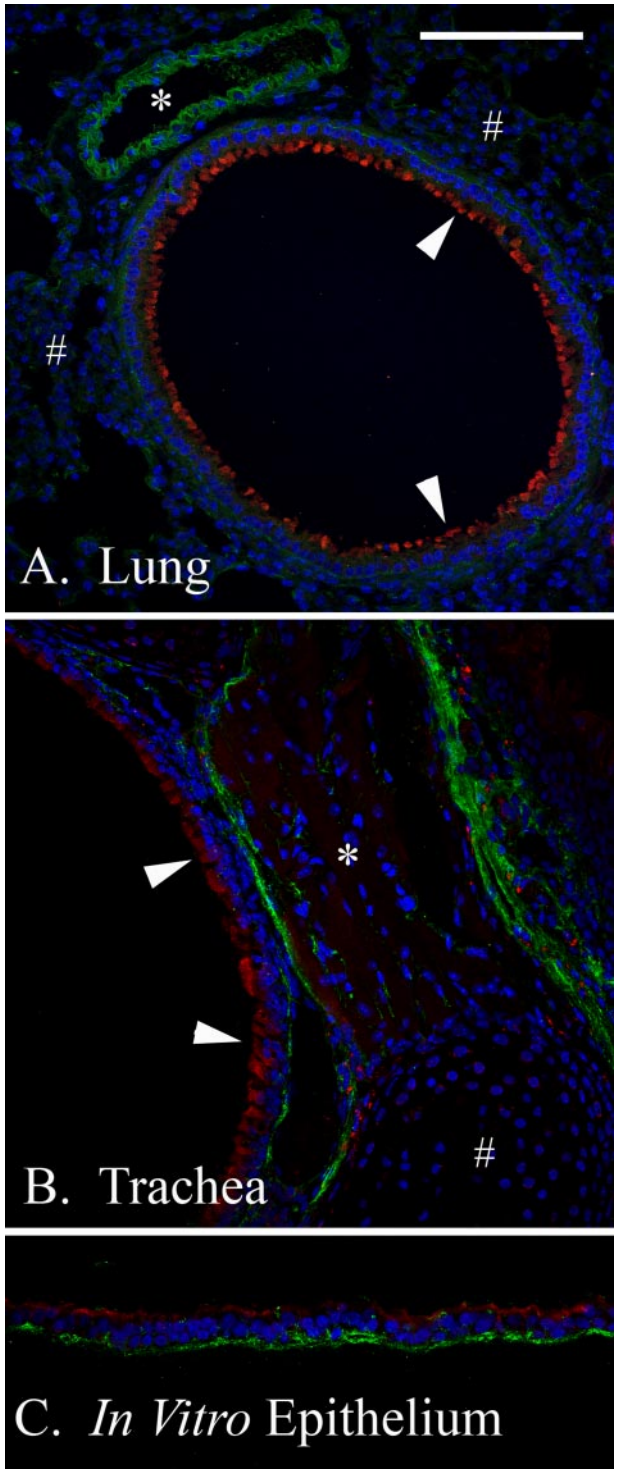

FIGURE 6. **KDEL and hyaluronan *in vivo* and *in vitro* airway distribution.** Paraffin sections from murine lung (*A*), trachea (*B*), or our *in vitro* differentiated airway epithelial model (*C*), were probed with an antibody against the tetrapeptide KDEL (*red*) and a hyaluronan-binding protein (*green*). Nuclei are *blue*. *In vivo* airway epithelial KDEL (*arrows*) presents higher expression than nearby alveolar cells (*pound signs*) or venules (*asterisk*) in the lung (*A*) as well as nearby smooth muscle cells (*asterisk*) or cartilage (*pound sign*) in the trachea (*B*). KDEL expression in our *in vitro*, differentiated AEC model (*C*) was similar to the trachea from which it was derived (*B*) (both the *green* and *red channels* were treated equally). Hyaluronan (*green*) distribution was primarily localized to the basal surface of the unstimulated AECs, with lesser quantities dispersed between the cells. Magnification is ×40. *Magnification bar*, 100 μm.

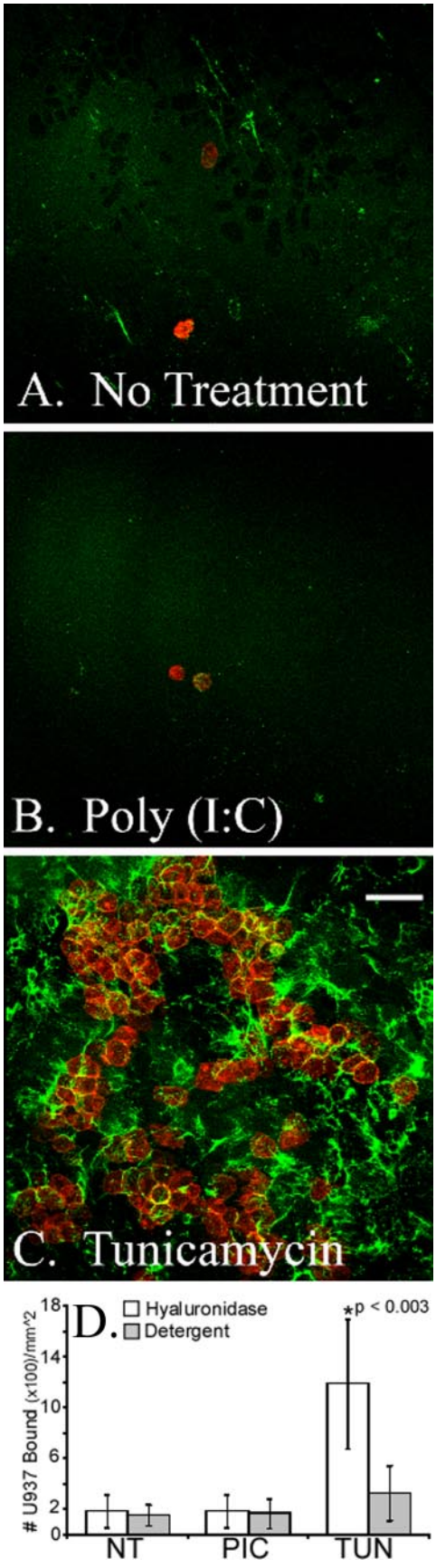

FIGURE 7. **U937 monocytic cells bind to hyaluronan on the apical surface of differentiated murine airway epithelial cells treated with tunicamycin.** CM-DiI-labeled U937 cells (*red*) were applied to the apical surface of epithelial cells treated without (*A*) or with poly(I,C) (*B*) or tunicamycin (*C*). After U937 binding and removal of unbound cells, hyaluronan (*green*) was labeled with fluorescence-tagged streptavidin on a biotinylated hyaluronan binding protein (at 4 °C), and confocal images were taken of the live cells within the first 30 min of exposure to room temperature. Magnification is ×40. *Magnification bars*, 100 μm. In parallel cultures, the CM-DiI-labeled U937 cells (bound to hyaluronan) were released by *Streptomyces* hyaluronidase digestion. U937 cells not released by hyaluronidase digestion were extracted with a detergent (1% Triton X-100 in PBS). The hyaluronidase (*white bars*) and detergent (*gray bars*) extracts were measured on a fluorometer, and the results are presented in *D* ($n = 5$ for experiments performed on five different days). *Error bars*, S.D.

venule endothelial cells (*asterisk*). Similarly, in the trachea (Fig. 6*B*), the airway epithelium (*arrowheads*) shows greater KDEL expression than nearby smooth muscle (*asterisk*) or cartilage (*pound sign*). Our *in vitro* airway epithelium (Fig. 6*C*) shows similar KDEL expression to *in vivo* airway tissues (Fig. 6, *A* and *B*). Airway epithelial hyaluronan (*green*) was primarily found at the basal surface of the unstimulated cells, with smaller quantities dispersed between the cells (Fig. 6, *A* and *B*). Hyaluronan distribution in our *in vitro* model (Fig. 6*C*) closely resembled its *in vivo* distribution (Fig. 6, *A* and *B*).

Leukocyte Adhesion to the Hyaluronan Matrix Produced by Airway Epithelial Cells in Response to ER Stress—Leukocyte adhesion is primarily mediated by hyaluronan in smooth muscle cells treated with poly(I,C) or tunicamycin (17, 18). Using the lipophilic carbocyanine dye CM-DiI, we fluorescently labeled U937 monocytic (macrophage precursor) cells (*red*) and applied them (at 4 °C) to the apical surface of differentiated AECs treated with poly(I,C) or tunicamycin. Subsequently, we applied a biotinylated hyaluronan-binding protein and fluorescent streptavidin (*green*) to the cells and analyzed the living cells via confocal microscopy (Fig. 7). Significant (~6-fold; $n = 5$, $p < 0.003$) U937 cell adhesion was observed when the epithelial cells were treated with tunicamycin (Fig. 7*C*) compared with cells treated with poly(I,C) (Fig. 7*B*) or untreated (Fig. 7*A*). U937 cell adhesion was quantified by releasing the bound, fluorescently labeled, U937 cells with *Streptomyces* hyaluronidase and measuring the released cells on a fluorometer (Fig. 7*D*). Thus, the hyaluronan-mediated adhesion of U937 cells to the apical surface of differentiated AECs in response to tunicamycin, but not poly(I,C), is consistent with the preferential activation of the unfolded protein response by the epithelial cells and the accumulation of hyaluronan on their apical surface (Figs. 4 and 5).

The confocal images in Fig. 7 were acquired under static conditions, while the cells were under a coverslip. By subjecting the U937 cells bound to hyaluronan on tunicamycin treated AECs to gentle flow (at 4 °C) in a custom-made flow chamber, we were able to get a better perspective of the three-dimensional nature of this leukocyte-hyaluronan interaction and to confirm the observations made during static conditions. A time lapse movie of this process can be found in (supplemental movie S8), whereas two representative images are found in Fig. 8. The majority (>90%) of hyaluronan-bound U937 cells (*white*; epithelial cells are *black*) in Fig. 8*A* were tethered to hyaluronan (not fluorescently labeled), as evidenced by their swaying movement under medium flow and their subsequent release by

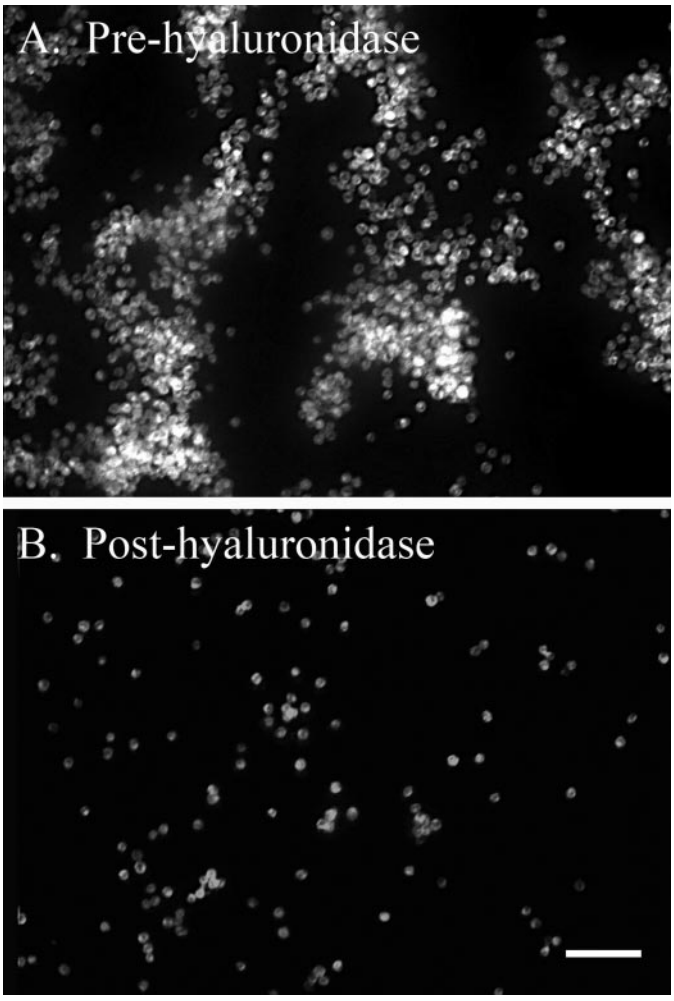

FIGURE 8. **U937 monocytic cells bound to hyaluronan on the apical surface of differentiated murine epithelial cells, treated with tunicamycin, are washed away following hyaluronidase digestion.** CM-DiI-labeled U937 cells (shown in *white*) were applied to tunicamycin-treated epithelial cells (shown in *black*) at 4 °C and subjected to gentle flow in a custom-made flow chamber. Images were taken (2 images/s) before (*A*) and after (*B*) hyaluronidase digestion (also at 4 °C). A movie of this process was generated, which illustrates the three-dimensional structure of the hyaluronan "cables" that readily bind the U937 cells (see supplemental movie S8). In the movie, a time stamp (*lower right*) can be used to follow the application of the hyaluronidase (~110 s) and the time at which the medium flow was resumed after the addition of the enzyme (~160 s). Magnification is ×10. *Magnification bar*, 100 μm. This experiment was repeated four times.

Streptomyces hyaluronidase (Fig. 8*B*). The movie of this process gives the viewer a unique three-dimensional perspective.

Leukocyte Mediated Degradation of the Hyaluronan Matrix Produced by Airway Epithelial Cells in Response to ER-Stress—In Fig. 8, the U937/epithelial co-culture was subjected to gentle flow while the flow medium was kept at 4 °C to slow down the metabolism of the U937 cells. In a parallel experiment, the initial flow medium was applied at 4 °C, displaying the swaying movement of the U937 cells (*white*; epithelial cells are *black*) tethered to hyaluronan (not fluorescently labeled) (Fig. 9*A*). Afterward, the 4 °C flow medium was replaced with medium equilibrated to 37 °C. Three min later (Fig. 9*B*), the hyaluronan matrix began to disorganize, as determined by the release of the activated U937 cells. Ten min after application of the 37 °C medium, most of the U937 cells had been washed

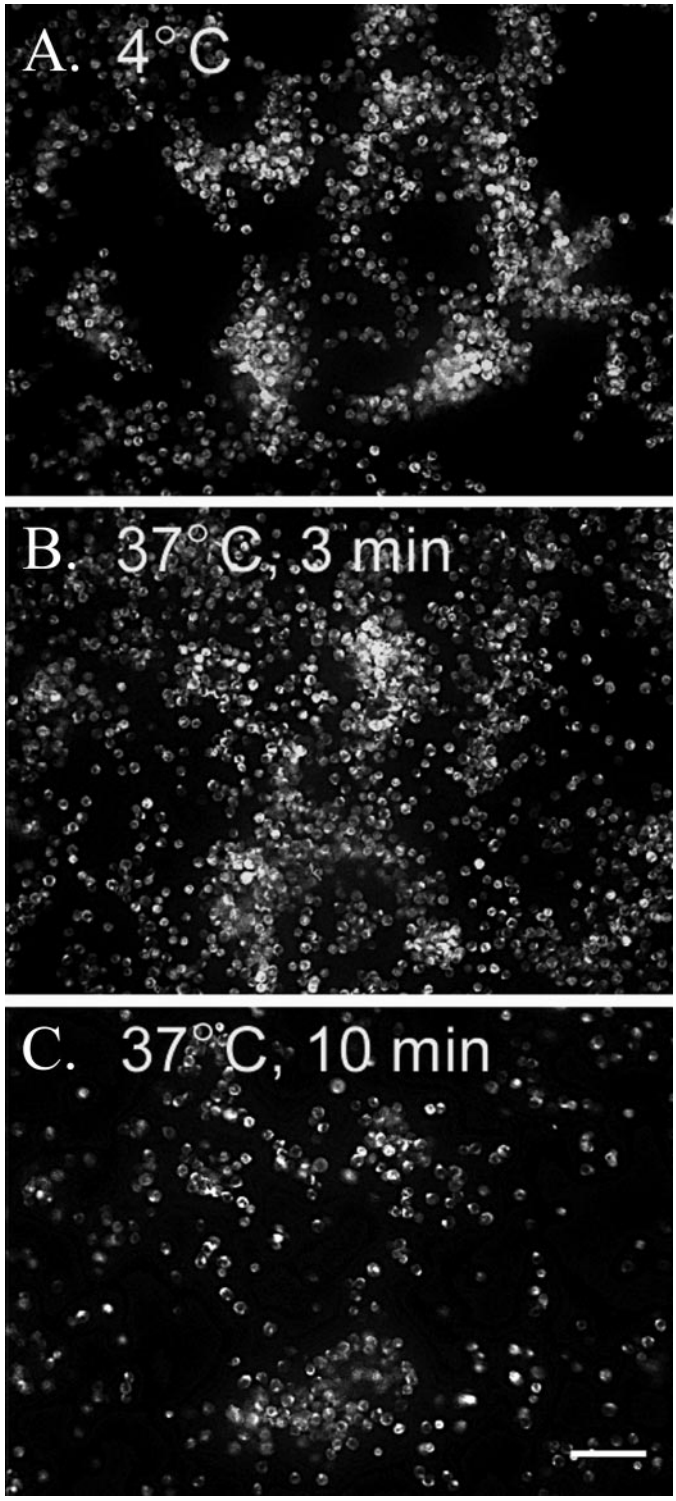

FIGURE 9. **U937 monocytic cells bound to hyaluronan on the apical surface of differentiated murine airway epithelial cells, treated with tunicamycin, are washed away when warmed to 37 °C.** Similar to Fig. 8, CM-DiI-labeled U937 cells (shown in *white*) were applied to the apical surface of tunicamycin-treated epithelial cells (shown in *black*) at 4 °C and subjected to gentle flow in a custom-made flow chamber. Images were taken (1 image/s) while the flow medium was kept at 4 °C for ~1 min (*A*) and subsequently switched to 37 °C medium for 3 min (*B*) and 10 min (*C*). A movie portraying the release of the U937 cells following this temperature shift was generated (see supplemental movie S9). In the movie, a time stamp (*lower right*) can be used to follow the application of the 37 °C medium (~150 s). Magnification is ×10. *Magnification bar*, 100 μm. This experiment was repeated three times.

away (Fig. 9*C*). The majority of remaining U937 cells were probably bound to other leukocyte adhesion molecules, such as the intercellular adhesion molecules (ICAMs) and lymphocyte function-associated antigens, although VCAM-1 does not appear to be involved (Fig. 5). When this temperature shift was attempted under static conditions (*i.e.* lacking flow), we observed that the U937 cells, instead of being released into the medium, slowly sank to the surface of the epithelial cells, and a significant portion attached to adhesion molecules on the epithelial cell surface, independent of hyaluronan (not shown). Such observations emphasize the need for medium flow in this type of experiment to remove hyaluronan-released U937 cells before they settle onto hyaluronan-independent adhesion proteins on the epithelial surface. A time lapse movie of Fig. 9 can be found in supplemental movie S9.

The spontaneous release of the U937 cells from the hyaluronan matrix at 37 °C suggested that the mechanism of release was via regional hyaluronan degradation at the site of contact between the U937 cell and the hyaluronan structure to which it was bound. In order to test this, we prepared the U937/epithelial cell co-culture in the same manner as described for Fig. 7 and took time lapse, three-dimensional, confocal *z*-scans every 5 min for 90 min total. Representative images of this process are presented in Fig. 10, and a time lapse movie can be found in supplemental movie S10. The cells were kept at 4 °C until imaged at room temperature. Minor activity was present during the first 30 min, presumably due to the suppressed metabolism of the cells. After 30 min at room temperature, we observed significant U937 cell (*red*) plasma membrane projections (*arrow* and *pound sign*) into the nearby hyaluronan matrix (*green*) during a time lapse from 0 (*A*) to 90 min (*B*). Briefly following the interaction of the U937 cell plasma membrane with the hyaluronan matrix, this matrix disappeared, suggestive of its degradation. Enlargements of these regions are presented in *C–F*. Also, during this time lapse, epithelium-derived hyaluronan matrix appeared to reorganize (compare *A* and *B*; *asterisk*) from an initial sheet of hyaluronan (*enlargement* in *G*) to a regionalized pattern outlining the tight junctions of the underlying epithelial cells (*H*; 90 min after exposure to room temperature). Since the hyaluronan matrix was coated with a fluorescence-labeled streptavidin bound to biotinylated hyaluronan binding protein, it is possible that the ability of the U937 cells to degrade hyaluronan was hindered. In parallel cultures lacking the hyaluronan-binding protein, similar U937 cell activity was observed (not shown). This activity appeared to be neither more nor less than the activity we observed when the hyaluronan matrix was labeled with the binding protein. In a separate experiment, primary murine peritoneal lavage macrophages, lymphocytes, and eosinophils were also shown to bind hyaluronan produced by the epithelial cells treated with tunicamycin (supplemental Fig. S3 and supplemental movie S11). In this experiment, regional hyaluronan degradation was followed by leukocyte migration through the regions where the hyaluronan matrix had been removed. These data provide the first real time, live imaging evidence that leukocytes can degrade the abnormal hyaluronan matrix induced when differentiated AECs are subjected to ER stress.

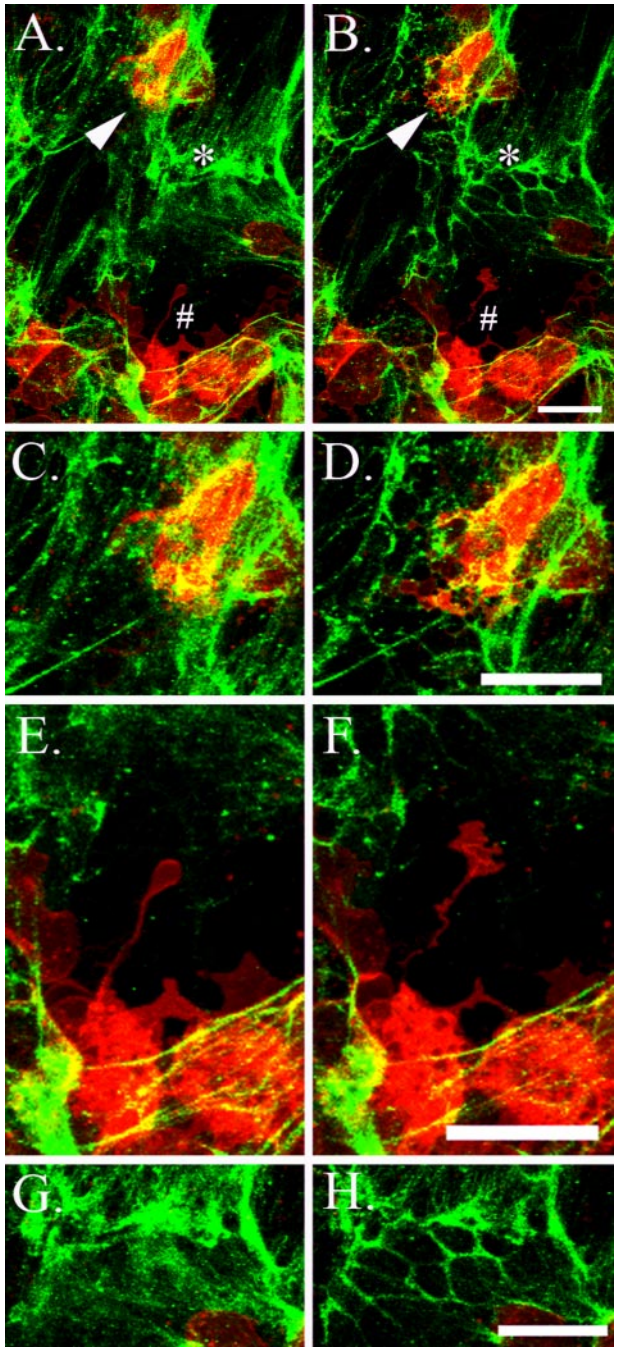

FIGURE 10. **U937 monocytic cells bound to hyaluronan on the apical surface of differentiated murine airway epithelial cells, treated with tunicamycin, degrade hyaluronan when warmed to 37 °C.** CM-DiI-labeled U937 cells (*red*) were applied to the apical surface of tunicamycin-treated epithelial cells (*black*) at 4 °C, and unbound cells were removed with gentle washing. Subsequently, hyaluronan (*green*) was labeled with fluorescence-tagged streptavidin on a biotinylated hyaluronan-binding protein, and confocal images were taken while the live cells were gradually permitted to reach room temperature. Three-dimensional *z*-scans were taken every 5 min (total 90 min), and a movie was generated from the maximized images (see supplemental movie S10). *Panels C* and *D*, *E* and *F*, and *G* and *H* are enlargements of regions marked by an *arrow*, *pound sign*, and *asterisk*, respectively, in *A* and *B*. The *left* and *right columns* present images taken at time 0 and 90 min after exposure to room temperature, respectively (except for *D*, which represents an image at 70 min to better illustrate the membrane protrusion of the U937 cell). These images show plasma membrane projections from the U937 cells into a nearby hyaluronan matrix (*D* and *F*). Afterward, the hyaluronan matrix is no longer visible, implying degradation. Also, we observed regions in which part of the hyaluronan matrix appears to be reorganized and concentrated around the epithelial cell junctions (compare *G* and *H*). *Magnification bars*, 25 μm. This experiment was repeated more than six times.

DISCUSSION

Most *in vitro* models of the differentiated airway epithelium involve seeding the cells onto a porous tissue culture insert precoated with collagen. Typically, this involves applying a rat tail type I collagen solution to the culture insert, incubating for a period of time, removing the excess solution, and permitting the residual collagen to air-dry (25). An alternative procedure employs a pH shift to form a rat tail native type I collagen gel with organized fibrils (23). Matrigel (BD Biosciences) is a commercial solution of BM components that could be used as a collagen substitute in this model. However, although it contains many of the unique BM components, an organized, quaternary structure between these matrix proteins is absent.

In the original description of the BM "lift culture" model (3), rat epidermal keratinocytes seeded onto this BM formed hemidesmosomes with the BM, whereas cells seeded onto the collagen substratum alone showed an irregular protrusion of the basal surface of the rat epidermal keratinocytes into the collagen substratum. It was also observed that cultures lacking a BM permitted the diffusion of hyaluronan into the supporting collagen layer.

In the present report, we described the application of murine, primary, airway, epithelial cells to the MDCK BM "lift culture" model first described by Tammi *et al.* (3). We showed that the BM significantly promoted AEC adhesion directly after seeding (Fig. 1, *A–D*). We also showed that the BM significantly promoted a smooth and regular basal epithelial surface in contrast to cells cultured on collagen alone (Fig. 1, *E* and *F*). Thus, culturing AECs on a native BM increased plating efficiency, produced better morphology, and resulted in an *in vitro* model that more closely resembles its *in vivo* counterpart.

Hyaluronan matrices, which promote leukocyte adhesion, have been shown to be produced in response to the following stimuli: poly(I,C) (17), tunicamycin (18), cycloheximide (18), dextran sulfate (18), high glucose (26), BMP-7 (27), and α_1-adrenergic receptor stimulation (28). These hyaluronan matrices have been shown to be produced by the following cells: primary colon smooth muscle cells (17), primary aortic smooth muscle cells (18), an immortalized proximal tubular epithelial cell line (27), primary mesangial cells (26), and an immortalized fibroblast cell line (28).

We examined the effect of poly(I,C) and tunicamycin on hyaluronan production (and leukocyte adhesion) by differentiated AECs. Similar to smooth muscle cells, tunicamycin treatment resulted in significant hyaluronan accumulation on the apical surface of the epithelial cells (Fig. 4) and the promotion of leukocyte adhesion (Fig. 7).

Interestingly, the AECs failed to increase hyaluronan synthesis (Fig. 4) or the expression of VCAM-1 (Fig. 5) in response to poly(I,C) despite doing so in smooth muscle cells (17). Since it is known that AECs express TLR3 (Toll-like receptor 3) on their apical surface (29), our unexpected result could imply that there is a signaling difference between the airway epithelial and smooth muscle cells downstream of TLR3. Alternatively, it is possible that the poly(I,C) induction of hyaluronan synthesis by smooth muscle cells functions independently of TLR3, perhaps through other double-stranded RNA receptors, such as RIG-1 (retinoic acid-inducible gene 1), MDA-5 (melanoma differentiation-associated gene 5) or PKR (double-stranded RNA-dependent protein kinase) (30). Unlike poly(I,C), tunicamycin does not require specific receptors for uptake by the cells. For technical and safety reasons, we chose not to infect the epithelial cells with a viable virus, but we suspect that this would induce a hyaluronan response similar to tunicamycin, if for no other reason than that viral infections are capable of inducing ER stress (19).

The significant accumulation of hyaluronan on the apical surface of AECs subjected to ER stress has implications for airway mucus composition and rheology. By confocal microscopy, we were unable to detect the presence of mucins, such as MUC 5AC, in the hyaluronan matrix induced by tunicamycin (not shown). This was not necessarily unexpected, considering the absence of goblet cells and secretory glands in our model. Thus, neither of these cell types was involved in the hyaluronan synthesis in this report. Since our *in vitro* model possessed both ciliated and nonciliated cells, the contribution of these two cell types to hyaluronan production is unclear. The U937 cell clusters in Figs. 8 and 9 imply that the hyaluronan matrix synthesized by the epithelial cells was regional in its distribution. Thus, we could speculate that only certain epithelial cells are responsible for the bulk of hyaluronan production. This may not necessarily involve the presence or absence of cilia but could be related to the cell division cycle, as has been reported for mesangial cells in reference to glucose-induced hyaluronan production (26). Regardless, it is possible that, in a typical human airway, ER stress would induce the apical synthesis of hyaluronan, resulting in significant, hyaluronan-rich, mucus production.

KDEL is a tetrapeptide on the carboxyl terminus of ER chaperone proteins (31). The significantly higher expression of KDEL in the unstimulated airway epithelium, compared with airway smooth muscle cells, was unexpected (Fig. 5). KDEL has been used as a reporter for ER stress (18), but it should be understood that KDEL-containing chaperones are proteins found in all normal cells that possess an ER. Furthermore, cells from different origins are likely to express different quantities of these chaperones, depending upon the extent of protein synthesis. For example, we would expect that cells with a well developed ER, such as plasma cells and pancreatic β cells, would express higher levels of KDEL-containing chaperones per cell than cells with a less developed ER. Thus, the relatively greater expression of KDEL in the airway epithelium, when compared with airway alveolar cells, venules, smooth muscle, and cartilage (Fig. 6), could be the result of a more developed ER in the epithelial cells, although this has not been described. For example, it is possible that routine maintenance of the tubulins involved in cilia motility on AECs could require a more robust protein synthetic machinery than that required for nonciliated cells. Another interpretation is that the AECs could routinely be under a certain amount of ER stress, greater than most other cell types. If this is true, it would imply that the airway epithelium could be particularly susceptible to pathogens or to genetic diseases, such as cystic fibrosis, familial hypercholesterolemia, and diabetes insipidus (32), which exploit the unfolded protein response.

The last part of this report focused on the interaction of a monocytic (macrophage precursor) cell line (U937 cells) with the apical hyaluronan matrix produced by the AECs in response to ER stress. The presence of viable leukocytes on the apical surface of the airway epithelium has been well established by their presence in bronchoalveoloar lavage from both normal and inflamed lungs (33). Pertinent to this study, increased numbers of mast cells, eosinophils, neutrophils, and monocyte/macrophages have been reported in bronchoalveolar lavage from asthmatics (34). Thus, the U937 cell interaction with the abnormal hyaluronan matrix on the apical surface of our AECs is a model consistent with what is known to occur *in vivo*.

We observed significant clusters of U937 cells tethered to a tunicamycin-induced matrix that were completely disrupted by hyaluronidase treatment (Fig. 8). Furthermore, when the metabolism of the U937 cells was permitted to operate at physiological temperature (37 °C), the U937 cells released themselves from the hyaluronan matrix (Fig. 9). In contrast, U937 cells attached directly to the epithelial cell surface (probably via hyaluronan-independent epithelial-leukocyte adhesion receptors) did not wash away under these conditions (Fig. 9*C*). The spontaneous release of the U937 cells from the hyaluronan matrix at 37 °C implied regional hyaluronan degradation at the site of contact between the U937 cells and the hyaluronan matrix.

We speculate that the initial adhesion of the U937 cells to the hyaluronan matrix (at 4 °C) was accomplished by one or more hyaluronan receptors on the U937 cell surface, such as CD44, RHAMM (receptor for hyaluronic acid-mediated motility), and/or HARE (hyaluronan receptor for endocytosis) (35). Regardless of the receptor(s) involved in the initial adhesion of the U937 cells, CD44 is probably fundamentally involved in the spontaneous release of the U937 cells from the hyaluronan matrix at 37 °C. This is supported by a study involving $CD44^{-/-}$ mice, which showed that, although $CD44^{-/-}$ macrophages were able to reach the site of inflammation in the murine bleomycin model of lung injury and repair, they were unable to remove the massive quantities of hyaluronan that had accumulated as part of the airway pathology. In contrast, bone marrow transplanted into irradiated $CD44^{-/-}$ mice rescued the wild type phenotype with removal of the hyaluronan by $CD44^{+/+}$ macrophages and the subsequent recovery of the mice (36).

Based on these observations, we expect CD44 to be significantly involved in the U937 cell membrane protrusion and apparent degradation of the airway epithelial hyaluronan matrix (Fig. 10). The protrusions of the U937 cell membranes and their structural alterations during this process directly corresponded with the structural changes of the hyaluronan matrix at the site of contact and the subsequent regional disappearance of that matrix. Since the disappearance of the hyaluronan matrix only occurred when the probing membranes of the U937 cells made contact with the hyaluronan matrix, this implies that the disappearance of the matrix was caused by enzymatic degradation at the cell surface of the U937 cells and not the result of a secreted hyaluronidase. The purpose of the U937 cell membrane protrusions appears to be directly related to removal of the hyaluronan matrix, considering that the protrusions receded following the disappearance of the hyaluronan matrix. The protrusion of the U937 cell membrane in (Fig. 10*D*) appears to maximize the amount of surface area that it can use to come into contact with the hyaluronan matrix, again emphasizing the likelihood that the hyaluronan degradation was accomplished via a hyaluronidase anchored in the plasma membrane. The more slender protrusion of the U937 cell membrane in (Fig. 10*F*) reveals regions of greater lipid density, as observed by the brighter red color in the part of the projection that comes into contact with the hyaluronan matrix. It is possible that the enzymatic complex involved in the degradation of this matrix resides in this lipid-dense region. Hyal-2 (hyaluronidase-2) might be part of this complex, since it is a glycosylphosphatidylinositol-anchored enzyme that has been implicated in catabolic pathways involving cleavage and uptake of hyaluronan coordinated with binding of hyaluronan to CD44 (5, 6).

The overall degradation of hyaluronan for the duration of this experiment (90 min) was a minimal percentage of the total present. In other words, the U937 cells in Fig. 10 only showed active interaction and degradation of the hyaluronan matrix at one pole of their surface, despite being surrounded by hyaluronan. This implies that the catabolic machinery responsible for hyaluronan degradation is not uniformly distributed along the entire plasma membrane but rather localized to one specific region. Probably, this catabolic complex in the plasma membrane is fluid, with the potential to be reorganized on a different region of the cell surface, as needed. Not all hyaluronan-bound U937 cells displayed protrusions with obvious hyaluronan degradation. Specifically, U937 cells in clusters with each other bound to hyaluronan were the least likely to protrude and degrade (not shown). On the other hand, not all isolated U937 cells presented these protrusions (perhaps ~20%). The circumstances that induce U937 cells to display the phagocytic response observed in Fig. 10 are not clearly understood. Removal of hyaluronan also corresponded with peritoneal lavage leukocyte trafficking, primarily by lymphocytes (supplemental Fig. S3 and supplemental movie S11).

We were also surprised to observe the apparent reorganization of the hyaluronan matrix from a generalized sheet of matrix to a regionalized matrix outlining the tight junctions of the epithelial cells (Fig. 10, *A* and *B*, *asterisk*; enlargement in *G* and *H*). We also observed this phenomenon in several other parallel experiments (not shown). We know that this transformation portrays matrix reorganization and not new synthesis, because newly synthesized matrix would not be labeled with the fluorescent hyaluronan probe. When a 90-min time lapse was done with AECs in the absence of the U937 cells, this matrix reorganization did not occur (not shown). This implies that the U937 cell interaction with the epithelial cells is driving the matrix reorganization, possibly by the release of cytokines from the U937 cells. Other investigators provide significant evidence that RHAMM is on the apical surface of differentiated AECs, despite the apparent absence of CD44 (37, 38). Thus, it is likely that this receptor plays a significant role in the reorganization of the hyaluronan matrix in our model.

Presumably, longer incubation times would result in further hyaluronan degradation, but the technical difficulties of this procedure precluded much longer incubation times than 90 min. These technical difficulties primarily involve the inability

to use an inverted microscope due to the unique culturing conditions of cells grown at an air-liquid interface, namely the opacity the collagen gel and the porous membrane of the culture insert. Thus, it is necessary to use an objective that approaches the cells from the side of the apical surface. For our purposes, this involved the placement of a coverslip on the apical surface. The primary disadvantages of this approach are that the coverslip has the potential to damage the cells, gas exchange is minimized, and the amount of medium that can be applied to sustain the cells during incubations longer than 90 min is minimal (<100 μl). On the other hand, cell types, such as smooth muscle cells, that can be readily cultured on a coverslip are suitable for inverted microscopy and could benefit the most from this live imaging approach. Regardless of these technical difficulties, this live confocal microscopy technique provides a unique perspective of the interaction between leukocytes and the abnormal hyaluronan matrix that accumulates on the apical surface of differentiated AECs in response to ER stress.

The role that this abnormal accumulation of hyaluronan on the apical surface of the airway epithelium might have in triggering or exacerbating asthma and chronic obstructive pulmonary disease is not yet known. Hyaluronan fragmentation is a well known by-product of inflammation, resulting from enzymatic and oxidative degradation by infiltrating leukocytes (39). These fragments have distinct biological activities when compared with macromolecular hyaluronan, including increased cilia beat frequency (13) and the induction of IL-8 and IL-10 (14) by the airway epithelium. The roles that these fragments might have in airway smooth muscle cell constriction or other aspects of airway hyperresponsiveness in asthma remain to be explored.

Acknowledgments—We acknowledge the kind support of Steven Brody (Department of Medicine, Washington University School of Medicine, St. Louis, MO) and Scott Randell (Department of Medicine, University of North Carolina, Chapel Hill, NC), who provided invaluable advice for culturing airway epithelial cells at an air-liquid interface. We also acknowledge Mei Yin (Imaging Core, Lerner Research Institute, Cleveland Clinic, Cleveland, OH) for help with the toluidine blue, "semithin" preparation of the epithelial cells. We also acknowledge the assistance of Jim Proudfit and Anthony Shawan (Prototype Laboratory, Lerner Research Institute, Cleveland Clinic, Cleveland, OH) for designing and building the custom flow chamber. Finally, we acknowledge the memory of Donald K. MacCallum, the original pioneer of the basement membrane lift culture model, whose valuable advice and sincere friendship were greatly appreciated throughout the initial phases of this project.

REFERENCES

1. Laitinen, A., and Laitinen, L. A. (1994) *Am. J. Respir. Crit. Care Med.* **150,** S14–S17
2. McCarthy, K. J. (2008) *Microsc. Res. Tech.*, **71,** 335–338
3. Tammi, R. H., Tammi, M. I., Hascall, V. C., Hogg, M., Pasonen, S., and MacCallum, D. K. (2000) *Histochem. Cell Biol.* **113,** 265–277
4. Weigel, P. H., Hascall, V. C., and Tammi, M. (1997) *J. Biol. Chem.* **272,** 13997–14000
5. Tammi, R., Rilla, K., Pienimaki, J. P., MacCallum, D. K., Hogg, M., Luukkonen, M., Hascall, V. C., and Tammi, M. (2001) *J. Biol. Chem.* **276,** 35111–35122
6. Stern, R., Kogan, G., Jedrzejas, M. J., and Soltes, L. (2007) *Biotechnol. Adv.* **25,** 537–557
7. Casalino-Matsuda, S. M., Monzon, M. E., Conner, G. E., Salathe, M., and Forteza, R. M. (2004) *J. Biol. Chem.* **279,** 21606–21616
8. Pirinen, R. T., Tammi, R. H., Tammi, M. I., Paakko, P. K., Parkkinen, J. J., Agren, U. M., Johansson, R. T., Viren, M. M., Tormanen, U., Soini, Y. M., and Kosma, V. M. (1998) *Int. J. Cancer* **79,** 251–255
9. Monzon, M. E., Casalino-Matsuda, S. M., and Forteza, R. M. (2006) *Am. J. Respir. Cell Mol. Biol.* **34,** 135–141
10. Sahu, S., and Lynn, W. S. (1978) *Biochem. J.* **173,** 565–568
11. Sahu, S., and Lynn, W. S. (1978) *Inflammation* **3,** 149–158
12. Hallgren, R., Samuelsson, T., Laurent, T. C., and Modig, J. (1989) *Am. Rev. Respir. Dis.* **139,** 682–687
13. Manzanares, D., Monzon, M. E., Savani, R. C., and Salathe, M. (2007) *Am. J. Respir. Cell Mol. Biol.* **37,** 160–168
14. Boodoo, S., Spannhake, E. W., Powell, J. D., and Horton, M. R. (2006) *Am. J. Physiol.* **291,** L479–L486
15. Casalino-Matsuda, S. M., Monzon, M. E., and Forteza, R. M. (2006) *Am. J. Respir. Cell Mol. Biol.* **34,** 581–591
16. Proud, D., and Chow, C. W. (2006) *Am. J. Respir. Cell Mol. Biol.* **35,** 513–518
17. de La Motte, C. A., Hascall, V. C., Calabro, A., Yen-Lieberman, B., and Strong, S. A. (1999) *J. Biol. Chem.* **274,** 30747–30755
18. Majors, A. K., Austin, R. C., de la Motte, C. A., Pyeritz, R. E., Hascall, V. C., Kessler, S. P., Sen, G., and Strong, S. A. (2003) *J. Biol. Chem.* **278,** 47223–47231
19. Dimcheff, D. E., Faasse, M. A., McAtee, F. J., and Portis, J. L. (2004) *J. Biol. Chem.* **279,** 33782–33790
20. Pahl, H. L. (1999) *Physiol. Rev.* **79,** 683–701
21. Kincaid, M. M., and Cooper, A. A. (2007) *Antioxid. Redox Signal.* **9,** 2373–2387
22. Haines, D. S., Strauss, K. I., and Gillespie, D. H. (1991) *J. Cell Biochem.* **46,** 9–20
23. You, Y., Richer, E. J., Huang, T., and Brody, S. L. (2002) *Am. J. Physiol.* **283,** L1315–L1321
24. Sundstrom, C., and Nilsson, K. (1976) *Int. J. Cancer* **17,** 565–577
25. Bals, R., Beisswenger, C., Blouquit, S., and Chinet, T. (2004) *J. Cyst. Fibros.* **3,** Suppl. 2, 49–51
26. Wang, A., and Hascall, V. C. (2004) *J. Biol. Chem.* **279,** 10279–10285
27. Selbi, W., de la Motte, C., Hascall, V., and Phillips, A. (2004) *J. Am. Soc. Nephrol.* **15,** 1199–1211
28. Shi, T., Duan, Z. H., Papay, R., Pluskota, E., Gaivin, R. J., de la Motte, C. A., Plow, E. F., and Perez, D. M. (2006) *Mol. Pharmacol.* **70,** 129–142
29. Koff, J. L., Shao, M. X., Ueki, I. F., and Nadel, J. A. (2008) *Am. J. Physiol. Lung Cell Mol. Physiol.*, **294,** L1068–L1075
30. Matsukura, S., Kokubu, F., Kurokawa, M., Kawaguchi, M., Ieki, K., Kuga, H., Odaka, M., Suzuki, S., Watanabe, S., Homma, T., Takeuchi, H., Nohtomi, K., and Adachi, M. (2007) *Int. Arch. Allergy Immunol.* **143,** Suppl. 1, 80–83
31. Munro, S., and Pelham, H. R. (1987) *Cell* **48,** 899–907
32. Jorgensen, M. M., Bross, P., and Gregersen, N. (2003) *APMIS* **109**, (suppl.) 86–91
33. Reynolds, H. Y. (2000) *Lung* **178,** 271–293
34. Smith, D. L., and Deshazo, R. D. (1993) *Am. Rev. Respir. Dis.* **148,** 523–532
35. Jiang, D., Liang, J., and Noble, P. W. (2007) *Annu. Rev. Cell Dev. Biol.* **23,** 435–461
36. Teder, P., Vandivier, R. W., Jiang, D., Liang, J., Cohn, L., Pure, E., Henson, P. M., and Noble, P. W. (2002) *Science* **296,** 155–158
37. Forteza, R., Lieb, T., Aoki, T., Savani, R. C., Conner, G. E., and Salathe, M. (2001) *FASEB J.* **15,** 2179–2186
38. Lackie, P. M., Baker, J. E., Gunthert, U., and Holgate, S. T. (1997) *Am. J. Respir. Cell Mol. Biol.* **16,** 14–22
39. Stern, R., Asari, A. A., and Sugahara, K. N. (2006) *Eur. J. Cell Biol.* **85,** 699–715